

Background

The accurate measurement of the color of surfaces using the human tristimulus models has proven to be a difficult task for researchers [4]. The reasons for this are many with the primary issues being the highly nonlinear conversion between color spaces, adequate spectral characterization of the illumination and sensor, and uniform perceptual based metrics. Added difficulties arise when these color measurements are made during the high-speed production of textiles with intricate printed patterns. Current industry practice requires that a segment of the material be removed (i.e., a “strike-off”) and taken to a lab containing a colorimeter or spectrophotometer. The time required for this analysis typically is too great to effect the production process in a timely manner, especially for those many manufacturers who produce short runs of fabric (e.g., 1000 to 3000 yards at 150 yards / minute = 7 to 20 minutes per run). In addition, the standard color measurement equipment averages all the color in a predefined region, such as a small (e.g., 3/8 in. to 5/8 in.) circle. The ITC system uses a vector-space and set theoretic approach to address the nonlinear optimization problem of transforming the measured component colors to the predicted tristimulus responses. Image processing techniques are used to segment regions based on the geometry of the printed patterns and generate statistical averages of the component colors within these segmented regions. The use of international standards such as CIELAB and ΔE_{CMC} for the color metrics provides a perceptual basis for all measurements. We address these issues using a machine vision approach. In a machine vision system the electronic camera and associated filters function as the viewer and the objective is to map the response of these two components to the ideal human tristimulus response with a standard illuminant. The advantages of using a machine vision solution in combination with new processing algorithms for measuring online process color variations over a traditional colorimeter or spectrophotometer are the ability to make repeatable color measurements for an arbitrary geometric shape during on-line inspection.

Colorimetry Fundamentals

In this section we will briefly review the fundamentals of colorimetry and describe the color metrics adopted for the ITC system development effort. Several references are available which review this subject in greater depth [1, 5, 6, 7, 8]. Early human color vision research performed by Grassmann and Maxwell theorized that color could be mathematically specified in terms of three independent components. This theory matched the hypothesis that the human eye contained three receptors, each with a unique spectral response function. It was shown that any additive color mixture could be matched by the proper amounts of three primary colors. This is commonly called the tristimulus response. Determining the amount of these primary colors that are required to match an unknown color can specify the human visual response. The Commission Internationale de l’Eclairage (CIE) used this fact to establish a standard for numerical specification of color in terms of three coordinate or tristimulus values (XYZ).

The tristimulus response of the human eye to a solid-colored object is a function of three physical attributes: the spectral reflectance of the object, the spectral content of the illumination source, and the spectral response of the viewer. The spectral response of the viewer is defined by the tristimulus response curves determined by the CIE. The tristimulus values are given by the following equation,

$$\{d_1, d_2, d_3\} = \int \{x_1(\lambda), x_2(\lambda), x_3(\lambda)\} E(\lambda) \rho(\lambda) d\lambda \text{ or } d = XE\rho, \quad (1)$$

where $E(\lambda)$ is the spectral response of the illumination, $\rho(\lambda)$ is the spectral reflectance of the object, and $\{x_1(\lambda), x_2(\lambda), x_3(\lambda)\}$ are the human tristimulus response curves. A colorimeter instrument has a spectral response that is different from the CIE-defined human spectral response and the resulting measured tristimulus values are given by,

$$\{c_1, c_2, c_3\} = \int \{r_1(\lambda), r_2(\lambda), r_3(\lambda)\} E(\lambda) \rho(\lambda) d\lambda \text{ or } c = RE\rho, \quad (2)$$

where $\{r_1(\lambda), r_2(\lambda), r_3(\lambda)\}$ represents the spectral responses of the three component color channels of the colorimeter. The primary objective of the nonlinear optimization is to derive a mapping that converts the vector c to d .

Several color spaces have been developed that attempt to define an n-dimensional space such that a given distance in the space corresponds to a uniform perceivable color difference. These color spaces are specified by formulas that relate the tristimulus values to coordinates in the new space. The color space used in this work is the CIE 1976 CIELAB for the 10° observer. A further refinement of the measurement of color difference is defined as ΔE_{CMC} [9]. This refinement attempts to establish a more uniform metric for describing color differences and has been adopted by in the textile industry. ΔE_{CMC} is defined by the following relationships that are used in this study,

$$\Delta E_{CMC(2:1)} = \sqrt{\left(\frac{\Delta L^*}{\ell S_L}\right)^2 + \left(\frac{\Delta C_{ab}^*}{c S_c}\right)^2 + \left(\frac{\Delta H_{ab}^*}{S_H}\right)^2} \quad (3)$$

where ΔL^* in the $L^*a^*b^*$ coordinate system is typically defined by,

$$\Delta L^* = 116 f\left(\frac{Y}{Y_o}\right)^{\frac{1}{3}} - 16 \quad \text{if} \quad \frac{Y}{Y_o} > 0.01 \quad (4)$$

or

$$\Delta L^* = 903.3 f\left(\frac{Y}{Y_o}\right) \quad \text{if} \quad \frac{Y}{Y_o} \leq 0.008856$$

and ΔC_{ab}^* and ΔH_{ab}^* are polar functions of the a^* (red/green) and b^* (blue/yellow) coordinates defined by,

$$a^* = 500 \left(f\left(\frac{X}{X_o}\right)^{\frac{1}{3}} - f\left(\frac{Y}{Y_o}\right)^{\frac{1}{3}} \right), \quad b^* = 200 \left(f\left(\frac{Y}{Y_o}\right)^{\frac{1}{3}} - f\left(\frac{Z}{Z_o}\right)^{\frac{1}{3}} \right) \quad (5)$$

Projection onto Convex Sets Approach

As stated in the previous section the fundamental task required to achieve an imaging colorimeter is to derive a mapping that converts the vector \mathbf{c} to \mathbf{d} , thus matching the CIE human tristimulus response. Many approaches have been proposed and used for this mapping with the most straightforward being a linear combination. This transform is sufficient in many cases, especially if the mapping only occurs in a limited region of the color space. For a more accurate mapping, the nonlinear nature of the transform must be taken into account. The primary methods used today are three-dimensional look-up tables [10], least-squares polynomials [11, 12], neural networks [13], and set theoretic approaches. In this research we use a set theoretic approach based on the POCS method. Set theoretic approaches differ from classical estimation in that the solution is not based on minimizing or maximizing a cost function but rather on finding a solution which satisfies all the prescribed constraints, i.e., an intersection of sets. In this work we will also use a linear transform method based on a linear regression algorithm to compare the POCS results in subsequent sections.

The use of set theoretic methods has been employed in several signal-processing applications such as image restoration, tomographic reconstruction, and spectral analysis. Youla [14] used POCS for image restoration and gives a thorough description of the mathematics and algorithms used. Trussell [15] used POCS to specify metamers under different illuminations and to design optimum color filters for scanners.

In this work we have adapted previous work in set theoretic methods through the definition of various applicable constraints. The fundamentals of the POCS method are based on linear vector space theory. A central principle of vector space theory is the definition of an inner product. In the development and application of the POCS algorithm the Hilbert space is used as the working space because it is a complete inner product space (i.e., a finite dimensional vector space with the standard dot product used for the inner product represents a Hilbert space). With this vector space defined, we can describe how the constraints are represented as a closed convex set. A convex set is a set C in the Hilbert space such that if $f, g \in C$ and if $0 \leq \alpha \leq 1$, then $h = \alpha f + (1 - \alpha) g \in C$. This definition is shown graphically in two dimensions in Fig. 1. In basic terms, all the points on a line between any two points in the set must also be in the set. One can also show that the nonempty intersection of any two closed convex sets is also closed and convex. A solution lies in the intersection of all the constraint sets and is obtained by sequentially projecting an initial estimate of the solution onto each constraint set. This intersection is achieved through an iterative algorithm that converges to the intersecting boundary between the defined constraint sets as represented in Fig. 2. For further implementation details of the POCS algorithm, see [3, 15].

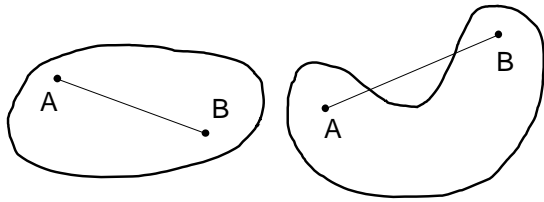


Figure 1 – A graphical representation of a convex set (left and a non-convex set (right).

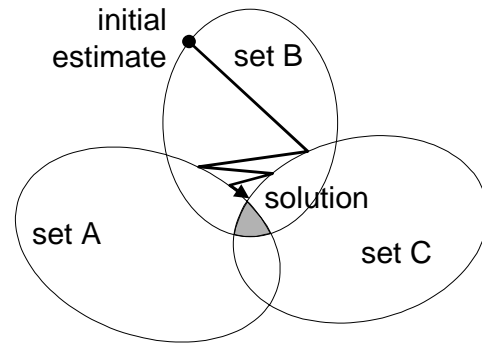
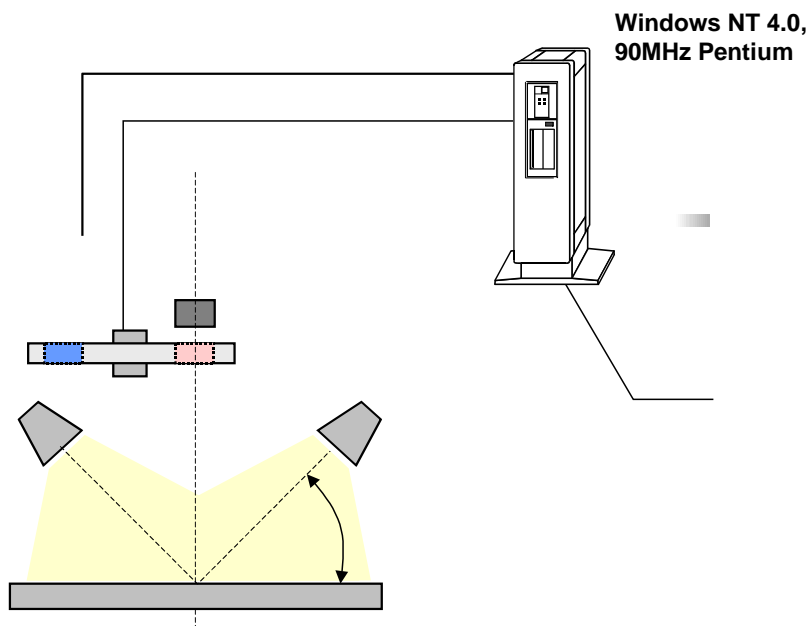


Figure 2 – A representation of the iterative projection operation that results in a solution along the boundary of the intersection of the constraint sets.

The ITC System

The ITC system developed for testing the POCS approach is shown schematically in Fig. 3. The ITC was developed as an offline system for developing and evaluating the POCS measurement approach. The product under inspection can be illuminated at various angles and illuminants. The illuminants used for this research were the MacBeth Sol Source D65 simulant based on a quartz-halogen lamp with custom filters, and a Pendant metal halide illuminant with a color temperature of 6500K.

The reflected energy was imaged through an Integrated Scientific color filter wheel onto a 768x484 CCD sensor in a Pulnix TM-9701 digital camera. The tristimulus filters in the filter wheel were selected to have the same general characteristics of the CIE tristimulus response curves and are shown in Fig. 4.



The digital Pulnix camera data was processed by a Matrox image processing board in a Windows NT, 90 MHz Pentium computer. A PC2000 plug-in PC spectrometer was used to measure the spectral characteristics of textile samples and calibration tiles. A Microsoft Visual basic graphical user interface (GUI) was developed to provide user access to the filter wheel, PC spectrometer, camera, and input and output data files. The image segmentation, data bookkeeping and tracking, and POCS algorithm were implemented in Microsoft Visual C++.

2. SEGMENTATION FOR COLOR ANALYSIS

The benefits of an imaging based colorimeter is the ability to make measurements on arbitrary shaped regions or objects. This section will describe the image processing algorithms used to segment and extract component colors (R in Eq. (2)) from regions within printed textile patterns. Many segmentation approaches exist and most fall into several broad categories such as local filtering (e.g. edge detection), snake and balloon methods, region growing and merging, and global optimization [16]. In this work during the first year, we initially took a global approach based on multilevel thresholds (i.e., a maximum entropy technique) derived from maximizing the contrast in a given color band [17]. While this approach performed reasonably well on most textile patterns, it did not take into account spatial information from the pattern under test. Consequently we have adopted a mean shift algorithm that iterates between a color-space clustering of the component colors and the spatial information across boundaries [18]. This is a simple, non-parametric method for estimating density gradients and can produce a high-quality edge image for color segmentation. The result is a more robust approach to discriminating between the various color regions in the image while filtering out border regions where color confusion will occur due to integration across discrete pixel boundaries or due to achievable tolerances in the rotary screen print process (e.g., overlapping of print). This procedure is indicated in Fig. 5.

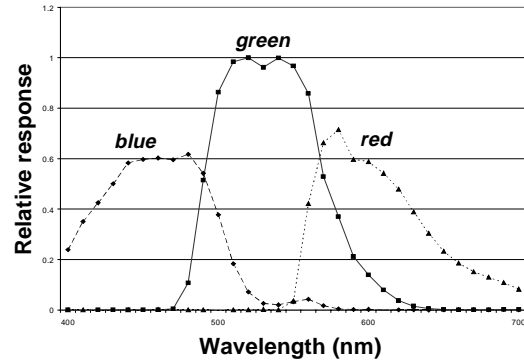


Figure 4 – Tristimulus spectral product (RE) of the ITC system.

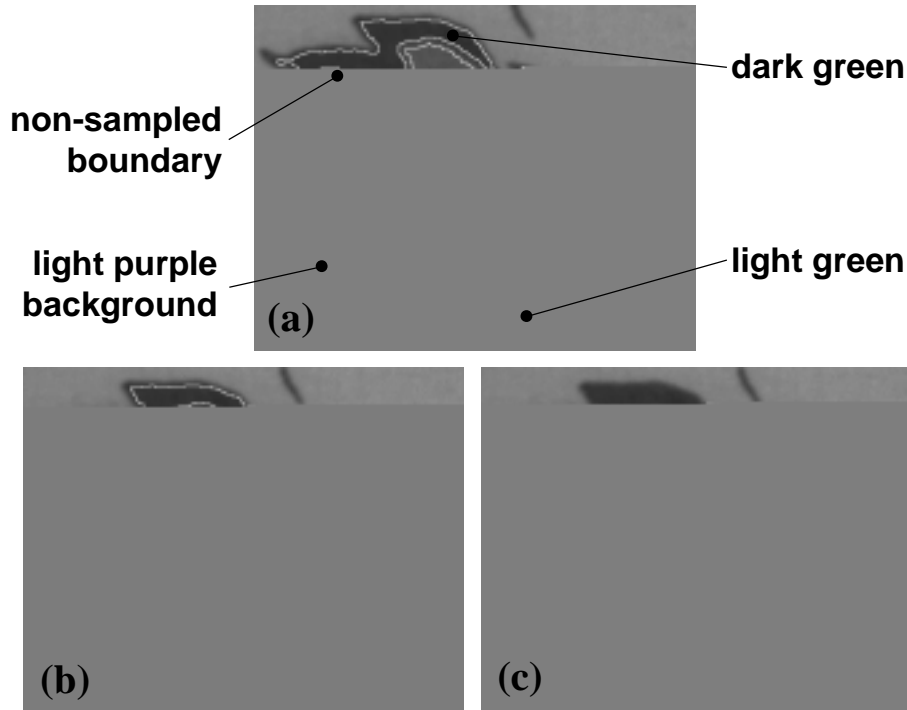


Figure 5 – Example of a textile pattern with three dominant colors, dark green (b), light green (c), and light purple (a). Note the excluded region of pixels between the boundaries in (a).

Figure 6 shows a flow diagram of the approach used by the ITC system for color segmentation. The first step is to perform a flat-field illumination correction and convert the component color of individual images to hue, lightness, saturation (HLS) or the $L^*u^*v^*$ color space, depending on whether the maximum entropy or mean shift algorithm is employed. This HLS or $L^*u^*v^*$ representation generates regions that correspond better to perceived boundaries than a solely intensity or raw component color segmentation. Next either the maximum entropy (first year effort) or mean shift algorithm (current work) is applied to the three component images. This process results in three labeled images that must then be post processed to identify and extract summary statistics from distinct regions. The first step in this post processing is to apply morphological erosion to each labeled region. This operation removes small noise generated regions and removes the boundary area of valid regions. The next processing step takes the intersection of the three labeled images to generate a composite labeled image.

The composite labeled image is then used to extract information from the original composite color images and provide it to the POCS algorithm. The average and standard deviation of the pixel values within a region are computed to generate the R vector and a statistical measure of the color uniformity within a region. In addition the centroid of each region is computed and used to look-up the initial estimate of the spectral reflectance, ρ , for the region.

3. ILLUMINATION

A complimentary rotary screen print inspection system was developed under the American Textile (AMTEX™) Partnership for pattern inspection and quality assessment as shown in Fig. 7 [19]. The on-line version of this system, designed by Sandia National Laboratory, uses a Dalsa tri-linear color line scan camera which requires a high-intensity illumination source (manufactured by Iridis) to achieve sufficient intensity for the rotary screen print process. The Iridis system uses a metal halide arc lamp in conjunction with an acrylic light pipe to deliver a focussed line source of illumination. Since the Iridis illumination system produces a line source, it was not suitable for testing with the ITC, but testing was required since a future on-line version of the ITC system will require a similar source to achieve sufficient exposure. Therefore an area illumination source manufactured by Pendant was obtained that had spectral characteristics similar to the Iridis.

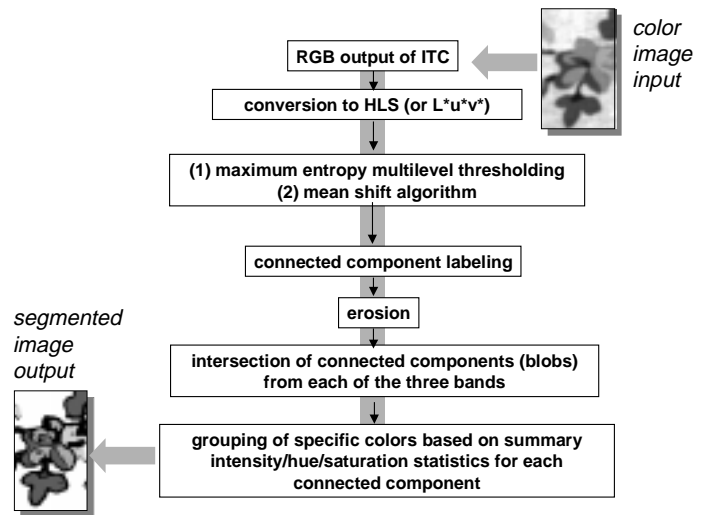


Figure 6 – Flow diagram of color region segmentation process.

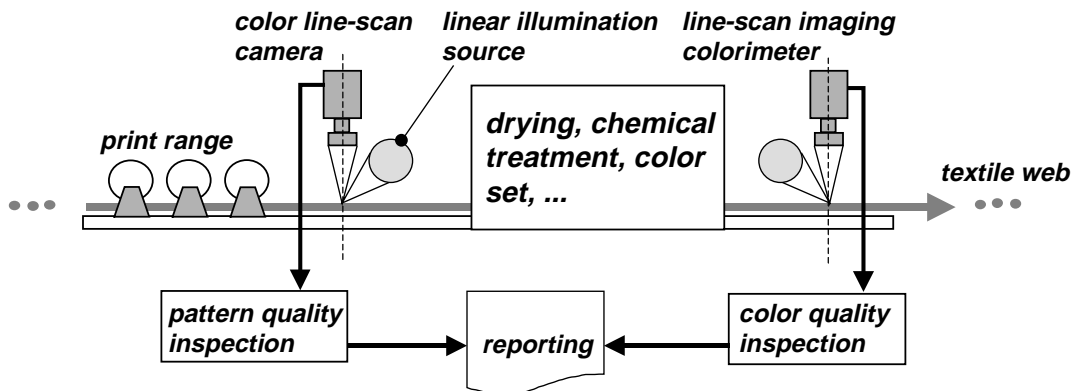


Figure 7 – Schematic representation of the rotary screen print pattern inspection system and imaging colorimetry system. Also shown are their relative positions in the manufacturing process.

The Sol Source (D65), Iridis (metal halide), and Pendant (metal halide) illumination spectrums are shown in Fig. 8. Note that the metal halide sources differ from the D65 illuminant in several important ways. For instance, the D65 illuminant, although fairly uniform, is dominated by energy at the blue end of the spectrum while the metal halide sources are dominant in the green region. Also, the D65 source is roughly equal in intensity across the spectrum varying by about 30% on average, whereas the metal halide sources vary as much as 90% and contain many peaks. The Pendant source is even more extreme in its variation across the visible spectrum than the Iridis source, therefore, we determined that this would be an overly conservative comparison and that the D65/Iridis system should compare even more favorably if the D65/Pendant system proved satisfactory.

One of the issues that needed to be addressed was related to the sample spacing used during the previous year's activities. The smoothly varying D65 illuminant and the smoothly varying spectral reflectance associated with textile colorants, required a sample spacing of no more than 10 nm to adequately represent the signals in the ITC system. If we sample the metal halide source at 10 nm intervals then important spectral detail is not maintained. We therefore increased the sampling by a factor of 10 (i.e., 1 nm samples) on all data processing in the ITC system. The improvement in spectrum fidelity for the metal halide illumination source is shown in Fig. 9.

4. RESULTS

The goal of the effort described herein was to determine the efficacy of using the metal halide illumination source to estimate the accuracy of a color difference measurement on textile products. Note that we seek to estimate color differences (e.g., ΔE_{CMC}), i.e., the variation of a target color over time from its original value, and not to compare absolute color measurements. To accomplish this goal we needed to determine a measurement technique to compare difference values obtained using POCS. A common technique for estimating colorimetric values from RGB color systems is to use a linear regression approach. Since we have a spectrometer embedded in the ITC system, it was possible for us to obtain standard CIE tristimulus measurements (i.e., XYZ) from a series of PantoneTM color samples independently of the RGB values put out by the color camera. Recall that the tristimulus vector was given in Eq. (1) by $\mathbf{d} = \mathbf{X}\mathbf{E}\rho$, where \mathbf{X} contains the tristimulus response curves for the CIE standard 10⁰ observer, \mathbf{E} contains the illumination spectrum, and ρ is the spectral reflectance of the color sample. A linear regression approach to transforming RGB to XYZ involves determining a transformation matrix, \mathbf{M} , such that $\mathbf{d} = \mathbf{M}\mathbf{c}$, where \mathbf{c} is a three-element vector that contains the RGB values that correspond to the XYZ values in \mathbf{d} . To determine \mathbf{M} , a series of color samples are measured such that a series of equations are obtained, $[\mathbf{d}_0 \ \mathbf{d}_1 \ \dots \ \mathbf{d}_{N-1}] = \mathbf{M} [\mathbf{c}_0 \ \mathbf{c}_1 \ \dots \ \mathbf{c}_{N-1}]$, for $N-1$

blue, brown, tan, rust, cool gray, and warm gray. The results of a comparison between POCS and the linear regression method are shown in Figs. 10 and 11 for the D65 and metal halide illuminants respectively. Note that each of the independent values along the bottom axis represent a shade pair, e.g., “green” refers to a pair of green Pantone™ color tiles of slightly varying shade. The solid line in these graphs represents a spectrometer color difference measurement that was taken to be the “standard” for this comparison. The standard in this case was a HunterLab Miniscan handheld spectrophotometer with its own self-contained D65 illuminant source. In Fig. 10, the regression and POCS results were both derived from the RGB values collected with the ITC under D65 illumination. In Fig. 11, the regression and POCS results were derived from the metal halide illuminant.

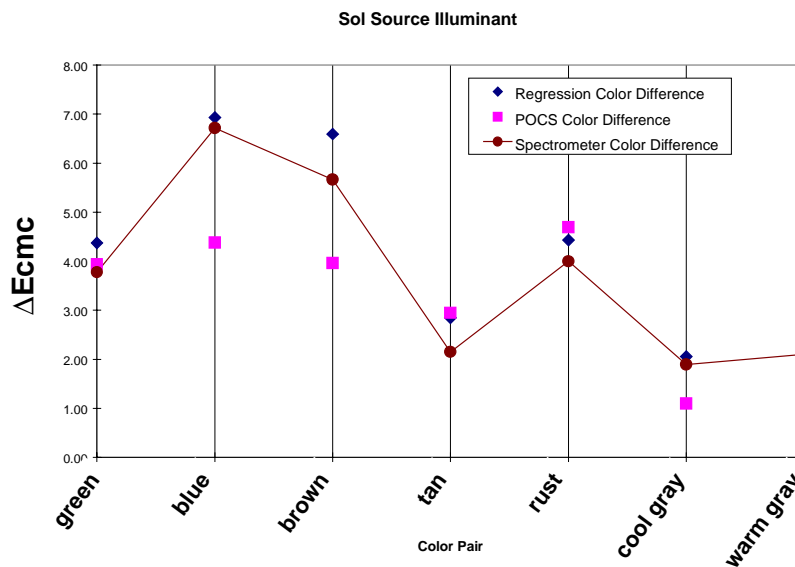


Figure 10 – Results of a shade difference comparison between the POCS technique, the linear regression method, and a standard spectrometer reading for D65 illumination.

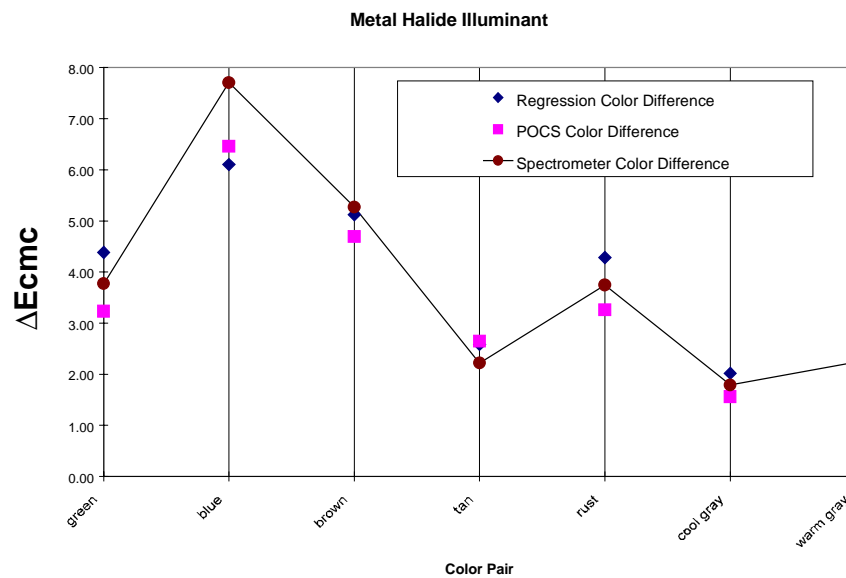


Figure 11 - Results of a shade difference comparison between the POCS technique, the linear regression method, and a standard spectrometer reading for metal halide illumination.

A calculation of the average magnitude difference between the spectrometer (standard) and the D65 data shown in Fig. 10 reveals the average error across all color pairs is $\pm 0.53 \Delta E_{CMC}$ units for the regression approach, while the POCS method resulted in an average error of $\pm 0.95 \Delta E_{CMC}$ units. For the metal halide illumination data shown in Fig. 11, the average error across all color pairs is $\pm 0.38 \Delta E_{CMC}$ units for the regression approach, while the POCS method resulted in an average error of $\pm 0.48 \Delta E_{CMC}$ units. Although the POCS results appear slightly less accurate than the regression technique, the difference between the two approaches is within the statistical significance of the numbers indicating that their performance is similar. The advantage to POCS comes from the ease of calibration and maintenance of the instrument in the field as will be described in the conclusions below.

Textile Color Tests

A final set of tests are reported in this section to determine the difference in colors from the beginning of a textile run to the end of a run for approximately 1,500 feet of printed fabric. The quantities of interest in an on-line measurement are related to the side-center-side color difference values in the cross-web direction and the beginning-of-run and end-of-run values in the web direction. Figure 12 shows the layout of positions on the fabric that were measured for this experiment.

There were three color samples that were evaluated during testing: a solid green background that covered large areas of the textile pattern, and smaller individual pink and blue regions whose object areas were no larger than 0.25 inch in diameter. In the case of the green background color, a laboratory spectrophotometer was used to determine a “standard” for comparison. We also used the PC spectrometer to measure a secondary “standard” that could be used with the smaller pink and blue regions. The spectrophotometer has a integrating field of view of approximately 1 inch and therefore encompasses too large an area for the smaller samples to be accurately measured. The PC spectrometer, on the other hand, can be focused to view a small region of the surface.

Figures 13, 14, and 15 show the results of comparing different positions across the web for the green, pink, and blue color samples respectively. In Fig. 13, a plot containing both the spectrophotometer and spectrometer are shown. Note the variability across the different detectors that is inherent in the color measurement process even between two spot detectors. When attempting to make absolute color difference measurements across different color measuring equipment, accurate agreement is difficult to obtain. Table I below summarizes the errors across the textile samples for the D65 and metal halide illuminations when compared to the PC spectrometer standard. For the green sample a comparison is also given for the spectrophotometer standard. Note overall for the PC spectrometer standard that the average ΔE_{CMC} error under D65 illumination is ± 0.29 while this error is ± 0.49 under metal halide illumination.

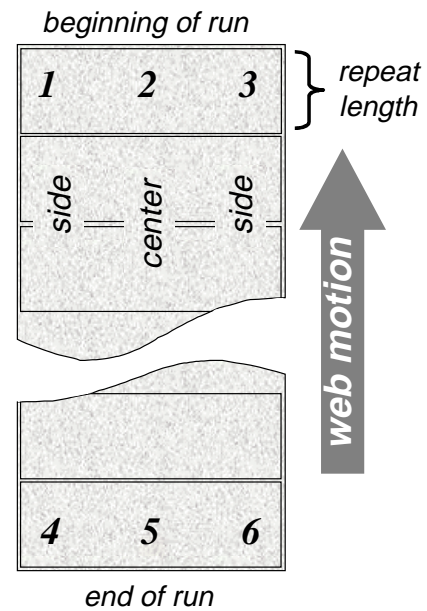
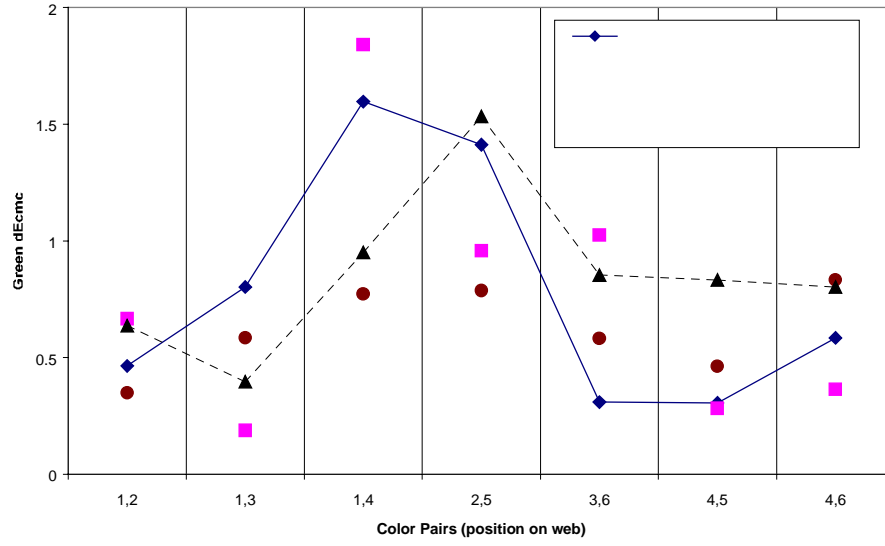


Figure 12 – Layout of textile fabric showing the side (1,4) center (2,5), side (3,6), and beginning of run (1,2,3), and end of run (4,5,6) positions on the fabric web

Table I – Summary of error across all textile samples versus illumination source. Error values are reported in ΔE_{CMC} units.

	Spectrometer vs. POCS Sol Source	Spectrometer vs. POCS metal halide	Spectrophotometer vs. POCS Sol Source	Spectrophotometer vs. POCS metal halide
Green (Fig. 13)	± 0.3	± 0.41	± 0.35	± 0.27
Pink (Fig. 14)	± 0.3	± 0.58	N/A	N/A
Blue (Fig. 15)	± 0.27	± 0.39	N/A	N/A

Textile Color Comparison (Green)



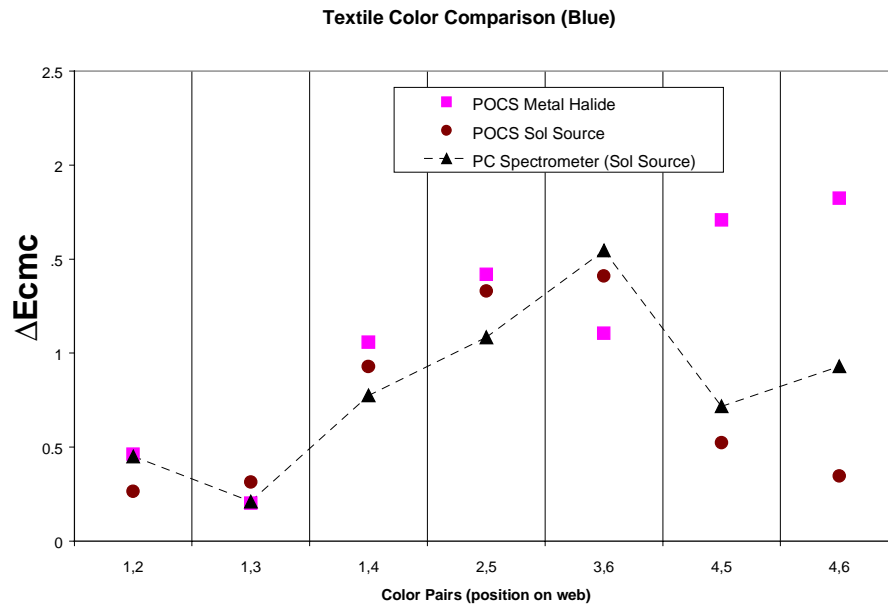


Figure 15 – Comparison of textile color “blue” under D65 and metal halide illumination.

5. CONCLUSIONS

In the field of machine vision inspection, it is necessary to balance many inspection system parameters with the realities of the manufacturing environment. During the first year of activities in the development of the POCS-based ITC system, a standard D65 illuminant was used to evaluate the image processing and colorimetry algorithms for suitability, stability, and robustness. To move the system closer to the on-line environment this past year, we introduced a spectrally complex, metal halide illumination source that was similar to what will be required in the textile-manufacturing process. We have presented the results of two experiments to compare the effect of D65 and metal halide illumination. A comparison was also made between the POCS-based color measurement method and standard linear regression for determining color differences.

When comparing linear regression techniques to POCS it should be noted that linear methods require recalibration with a large number of color samples if the system is to accurately measure color in other regions of the potential product color-space. The POCS algorithm, on the other hand, only requires a seed value (i.e., a spectral estimate) for the color under test, which can be easily provided from the textile die formulation system. This seed value can be supplied to the POCS-based system across the color gamut of the products to be inspected. If the illumination changes or drifts over time (e.g., with temperature or the age of the lamp), the regression technique must be recalibrated with the set of color samples. The POCS-based system only needs to recalibrate the illumination (e.g., which can be easily accomplished in-situ with the spectrometer and a BaSO_4 target such as that used with the ITC system). In general, once the ITC components have been characterized, only the illumination and seed value need ever be recalibrated.

The average error (in ΔE_{cmc} units) reveals that under both D65 or metal halide illumination the regression and POCS approaches are roughly equal in performance for the calibration tiles and color pairs used (i.e., ± 0.53 vs. ± 0.95 respectively for D65, and ± 0.38 vs. ± 0.48 respectively for metal halide). It should also be noted that the seed value approach to the POCS method provides correlation between the ITC and any other “standard” color measurement device used. Regarding the textile samples tested, we were able to show for the PC spectrometer standard that the average ΔE_{cmc} error under D65 illumination was ± 0.29 (which is consistent with the average error of ± 0.26 reported in [3]), while this error was ± 0.49

under metal halide illumination. Therefore, even under the extreme difference of the metal halide illuminant, the metal halide lamp degraded the overall performance of the system by roughly 1.5.

6. ACKNOWLEDGEMENTS

The authors would like to express their thanks to the U.S. Department of Energy, the AMTEXTM Partnership and the Textile Manufacturers who have participated in the Computer Assisted Fabric Evaluation Program (CAFÉ) since 1992. These textile companies continuously dedicated their time, resources, and expertise to the program over the duration, making it possible for us to learn and understand the manufacturing process and pursue this research and development. We would also like to thank Hunter Labs of Reston, Virginia, for their continued interest and support of the imaging tristimulus colorimeter development effort, specifically Marty Goldberg whose participation in CAFÉ industry review meetings and frequent visits to Oak Ridge were greatly appreciated.

7. REFERENCES

- [1] C.J. Bartleson, "Introduction," *Optical Radiation Measurements, Vol. 2, Color Measurements*, edited by F. Grum and C.J. Bartleson, Academic Press, New York, 1980, pp. 1–9.
- [2] CIE, "International Lighting Vocabulary," 3rd ed., Publ. No. 17 (E-1.1), Bureau Central CIE, Paris, 1970.
- [3] M.A. Hunt, J.S. Goddard, K.W. Hylton, T.P. Karnowski, R.K. Richards, M.L. Simpson, K.W. Tobin, and D.A. Treece, "Tristimulus Color Measurement of Printed Textile Patterns Using the POCS Algorithm", IS&T/SPIE's 11th International Symposium on Electronic Imaging: Science and Technology, San Jose Convention Center, January 1999.
- [4] A. R. Robertson, A. Staniforth, D.S. Gignac, and J. McDougall, "A Computer-Controlled Photoelectric Tristimulus Colorimeter," NRC Report Pro-387, Ottawa, 1972.
- [5] G. Wyszecki and W. S. Stiles, *Color Science: Concepts and Methods, Quantitative Data and Formulae*, 2nd ed., John Wiley and Sons, New York, 1982.
- [6] D. L. MacAdam, *Color Measurement: Theme and Variations*, 2nd ed., Springer-Verlag, New York, 1985.
- [7] R. S. Hunter and R.W. Harold, *The Measurement of Appearance*, 2nd ed., John Wiley and Sons, New York, 1987.
- [8] Gaurav Sharma and H. Joel Trussell, "Digital Color Imaging," *IEEE Trans. Image Processing*, Vol. 6, No. 7, pp. 901 – 932, July 1997.
- [9] *AATCC Technical Manual*, Vol. 69, pp. 326 – 329, American Association of Textile Chemists and Colorists, Research Triangle Park, NC, 1994.
- [10] P.C. Hung, "Colorimetric calibration in electronic imaging devices using a look-up table model and interpolations," *J. Electronic Imaging*, Vol. 2, pp. 53 – 61, Jan. 1993.
- [11] H.R. Kang, "Color scanner calibration," *J. Imaging Sci. Technol.*, Vol. 36, pp. 162 – 170, Mar./Apr. 1992.
- [12] G.D. Finlayson and M.S. Drew, "Constrained least-squares regression in color spaces," *J. Electronic Imaging*, Vol. 6, No. 4, pp. 484 – 493, Oct. 1997.
- [13] H.R. Kang and P.G. Anderson, "Neural network applications to the color scanner and printer calibrations," *J. Electronic Imaging*, Vol. 1, pp. 125 – 134, Apr. 1992.
- [14] D.C. Youla and H. Webb, "Image Restoration by the Method of Convex Projections: Part 1 – Theory," *IEEE Trans. Medical Imaging*, Vol. MI-1, No. 2, pp. 81 – 94, Oct. 1982.
- [15] H.J. Trussell, "Applications of Set Theoretic Methods to Color Systems," *Color Research and Applications*, Vol. 16, No. 1, pp. 31 – 41, February 1991.
- [16] S.C. Zhu and A. Yuille, "Region Competition: Unifying Snakes, Region Growing, and Bayes/MDL for Multiband Image Segmentation," *IEEE Trans. Pattern Analysis and Machine Intelligence*, Vol. 18, No. 9, pp. 884 – 900, Sept. 1996.
- [17] R. Kohler, "A Segmentation System Based on Thresholding", *Computer Graphics and Image Processing*, Vol.15, pp.319 – 338, 1981.
- [18] D. Comaniciu, P. Meer, "Robust Analysis of Feature Spaces: Color Image Segmentation", *Proc. IEEE Conf. On Computer Vision and Pattern Recognition*, Puerto Rico, June 1997, pp. 750-755.
- [19] *Vision Systems Design Magazine*, "On-line Textile-inspection System Uses Off-the-shelf Components", October 1999.